Expanded View Figures

Figure EV1. Generation of PI4K2A K/O cells and contribution of PI4K2A, PI4K2B, and PI4KB to late endosomal PI4P.

A Sequence analysis of the targeted region in PI4K2A K/O #20 or #26 cells created with CRISPR/CAS9 genome editing system. The cartoons showing the altered sequences were captured from Benchling (https://benchling.com/).

B The effect of PI4K2A K/O on the expression level of PI4KB and PI4K2B. Whole-cell lysates prepared from wild-type or the PI4K2A clones were subjected to Western blot analysis using anti-PI4K2A, anti-PI4KB, anti-PI4K2B, and anti-alpha-tubulin antibodies.

C Representative BRET measurement showing the relative amount of PI4P in Rab7- and Rab4-positive endosomes. The BRET analysis was performed using the P4M2x-Rab7 sensor as described in Fig 1C and D or by using P4M2x-Rab4 sensor in which the Rab7 was replaced by the Rab4 sequence. A1 inhibitor was added to the cell following baseline measurement. The result shown is from an experiment performed in triplicates. The graph shows normalized BRET values where the averages of triplicate measurements of A1-treated cells were divided by the averages of triplicates obtained in DMSO-treated controls.

D A BRET analysis was performed with the P4M2x-Rab7 probe as described in Fig 1D. To inhibit PI4KB, 300 nM of PIK93 was added together with 30 nM of A1 following baseline measurements.

E Wild-type or PI4K2A K/O clone #20 cells were transfected with control siRNA or one targeting PI4K2B. Western blot analysis was performed with anti-PI4K2B, anti-PI4K2A, and anti-alpha-tubulin antibodies 3 days after the transfection.

F A BRET analysis measuring late endosomal PI4P in cells after PI4K2B was knocked down in wild-type or PI4K2A K/O cells. The values in (D) and (F) were measured in the same 96-well plate but plotted separately for clarity (therefore, the blue curves are the same in the two panels). The BRET ratios were expressed relative to those of DMSO-treated control cells, and means ± SEM are shown from three experiments performed in triplicates.

Source data are available online for this figure.

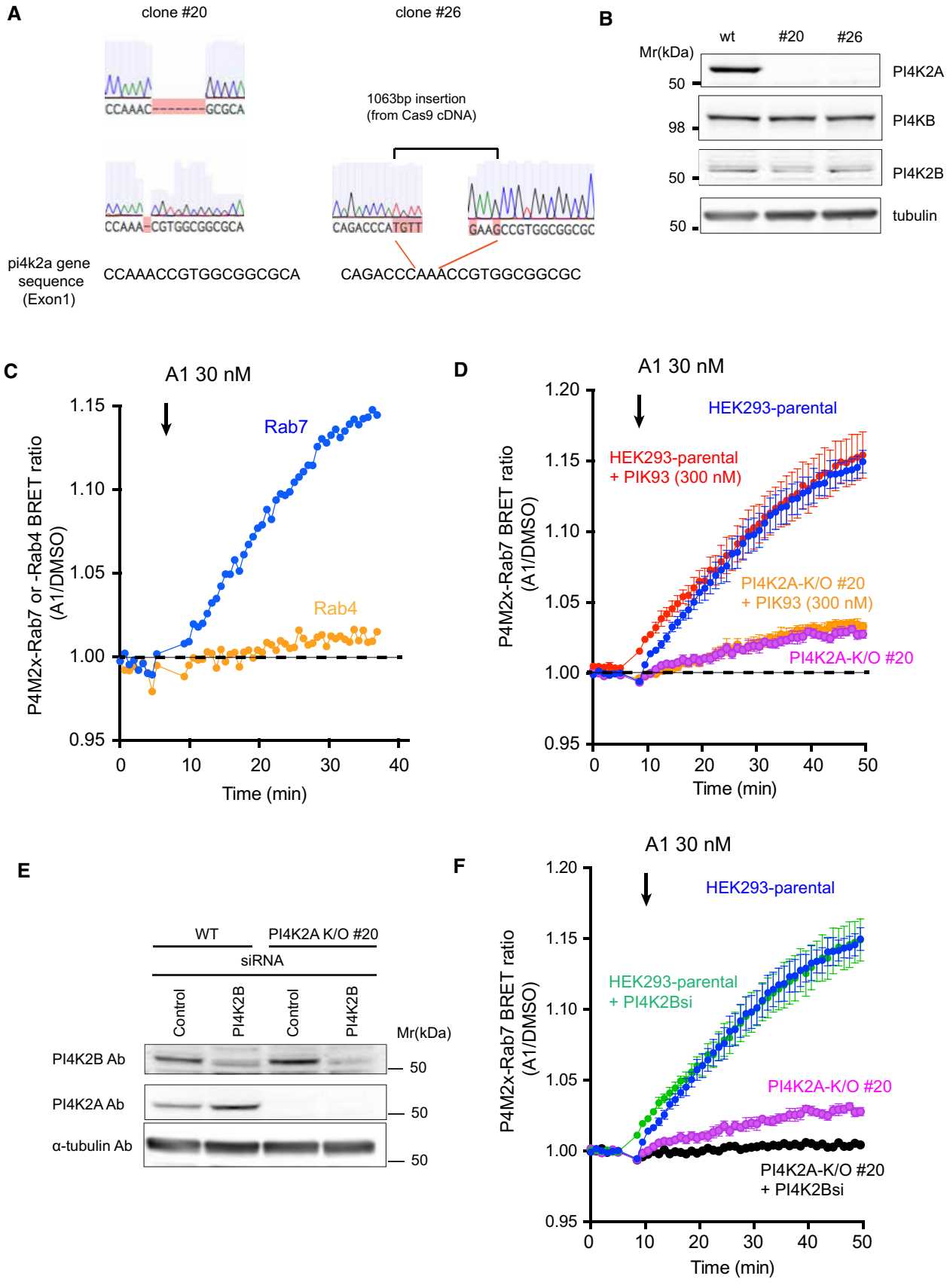

Figure EV1.

Figure EV2. Pull-down assays measuring the active state of Rab7 do not show apparent changes in PI4K2A K/O cells.

A Pull-down assays were performed as described in Materials and Methods using lysates prepared from wild-type or PI4K2A K/O cells #20 in which PI4K2B was knocked down by two different siRNAs (obtained from QIAGEN or GE). Whole-cell lysates were collected 3 days after the transfection and active Rab7 captured by the Rab7-GTP interacting motif of RILP. Western blot analysis of the captured material was performed with anti-Rab7, anti-PI4K2B, and anti-alpha-tubulin antibodies.

B Pull-down assays showing the amount of overexpressed Rab7 wild-type, N125I, Q67L mutant captured by the Rab7-GTP binding domain.

C Increased production of $PI(4,5)P_2$ in the Rab7 compartment by a recruited PIP5Kγ enzyme measured by BRET analysis in control and PI4K2A K/O cells. This panel originates from the same experiments shown in Fig 3C plotted separately for clarity (therefore, blue control curves are the same). For experimental details, see legend to Fig 3C. Means $\pm$ SEM from three separate experiments each performed in triplicates.

D This bar diagram shows the areas below the curves calculated from the time of rapamycin addition for each of four separate experiments similar to those shown in panel C (means $\pm$ SEM, $n = 4$). One-way ANOVA with Dunnett's multiple comparisons was used for statistical analysis (*$P = 0.0204$; **$P = 0.0081$).

E Knockdown (kd) of PI4K2B further reduces the amount of $PI(4,5)P_2$ generated by a recruited PIP5Kγ in the Rab7 compartment. This experiment was performed similarly to that shown in Fig 3E using the Rab7-QL mutant in the BRET construct. Means $\pm$ SEM from three separate experiments each performed in triplicates.

F Quantitation and statistical analysis of data shown in panel (E) performed as described for panel (D) (*$P = 0.0118$; **$P = 0.0023$).

Source data are available online for this figure.

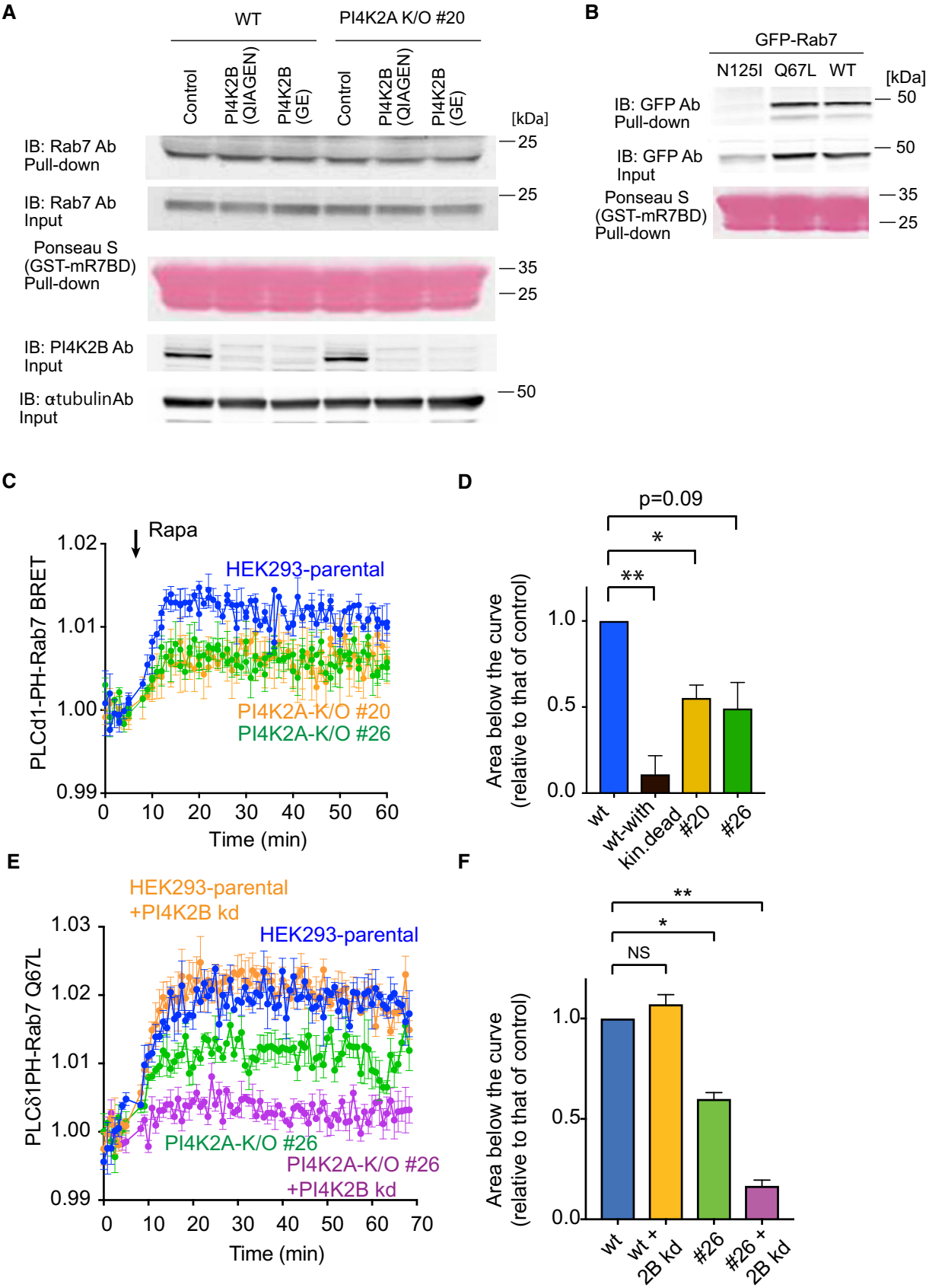

Figure EV2.

Figure EV3. Knockdown of PIP5Kβ and PIP5Kγ did not affect the level of PIP5Kα or plasma membrane PI(4,5)P_2.

A, C Western blot analysis with two different PIP5Kβ antibodies (AB1- or AB2-PIP5Kβ) performed with whole-cell lysates prepared from wild-type cells or from cells expressing myc- or mRFP-tagged PIP5Kβ. Note that both antibodies detect the expressed proteins but failed to detect the endogenous PIP5Kβ.

B siRNA against PIP5Kβ is effective as assessed by Western blotting using a GFP-humanPIP5Kβ enzyme. The amounts of transfected PIP5Kβ plasmid DNA are indicated.

D Western blot analysis showing the lack of effect of PIP5Kβ or PIPK5γ siRNA on the amount of PIP5Kα.

E BRET analysis showing the level of changes in plasma membrane PI(4,5)P_2 during stimulation by AngII in cells depleted in PIP5Kβ or PIPK5γ. AngII was added to the cells for monitoring the rate of PI(4,5)P_2 breakdown and subsequent re-synthesis. The BRET ratios were expressed relative to those of DMSO-treated cells, and means ± SEM are shown from three experiments performed in triplicates.

Source data are available online for this figure.

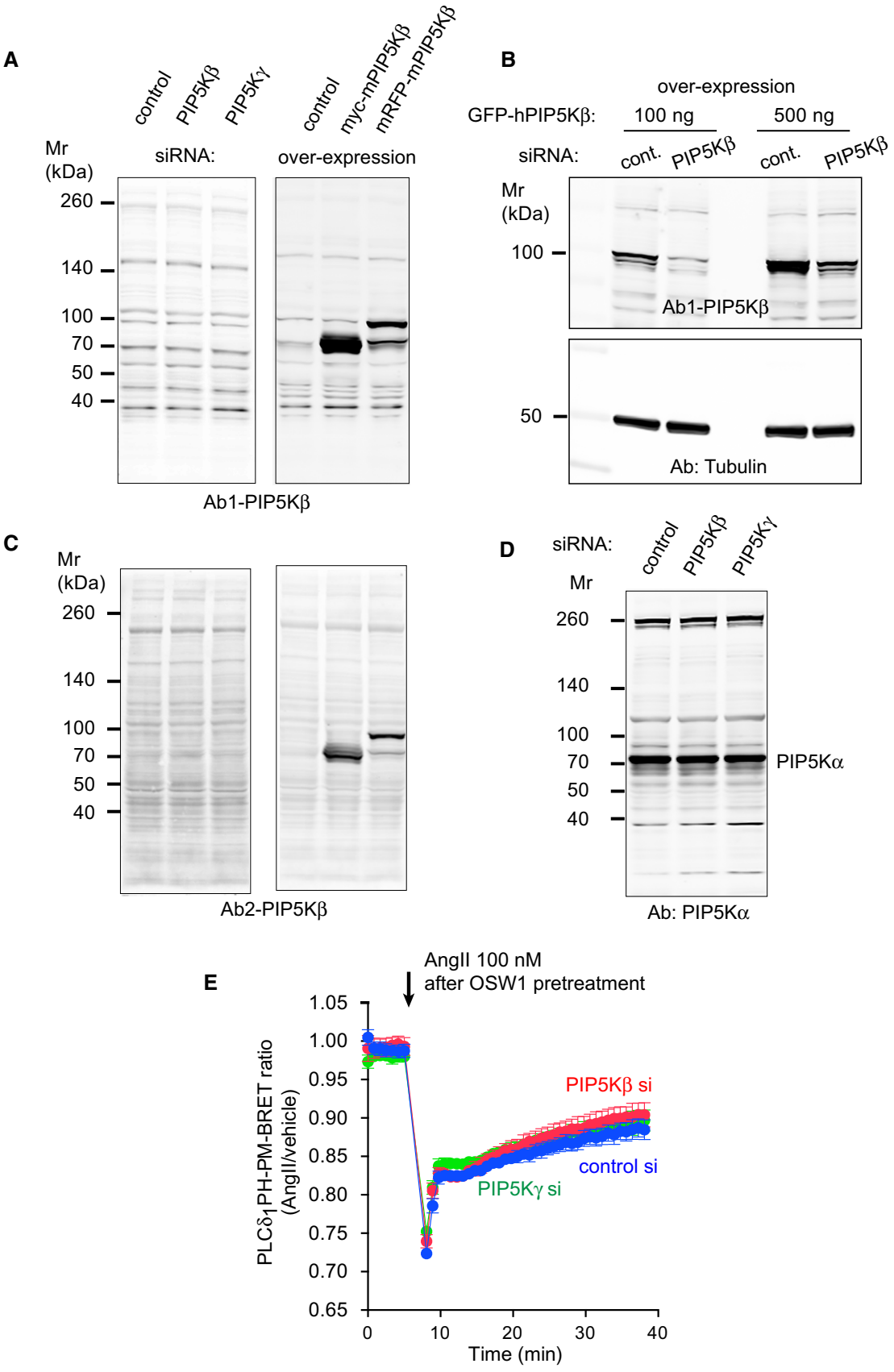

Figure EV3.

Figure EV4. $PI(4,5)P_2$ production releases the PLEKHM1 RH domain from Rab7-positive compartments.

A BRET analysis was performed as described for Fig 7C except that the RH domain of PLEKHM1 instead of the full-length PLEKHM1 protein was used in the BRET construct. Recruitment of PIP5Kγ to the Rab7 endosomes caused dissociation of the RH domain from late endosomes. This response was larger in wild-type cells than in PI4K2A K/O #20 cells. Means ± SEM from three separate experiments each performed in triplicates.

B BRET analysis showing that when Rab7Q67L mutant was used in the BRET construct it failed to release either the full-length PLEKHM1 or its RH domain from late endosomes when $PI(4,5)P_2$ was acutely produced. CFP(W66A)-FKBP-PIP5Kγ and iRFP-FRB-Rab7 was used as the recruitment constructs and Sluc-fused full-length PLEKHM1 or its RH domain together with Venus-tagged Rab7wt or Q67L mutant as the BRET sensor. Means ± SEM from three separate experiments each performed in triplicates.

C, D Live-cell confocal imaging showing the distribution of GFP-RILP or GFP-Vps35 upon acute production of $PI(4,5)P_2$ in the Rab7 compartment. HEK293-AT1 cells were transfected with CFP-FKBP-PIP5Kγ, iRFP-FRB-Rab7, and GFP-RILP(C) or GFP-Vps35(D). Next day, the images were captured by confocal microscopy before and after 100 nM rapamycin treatment. Scale bars: 20 μm.

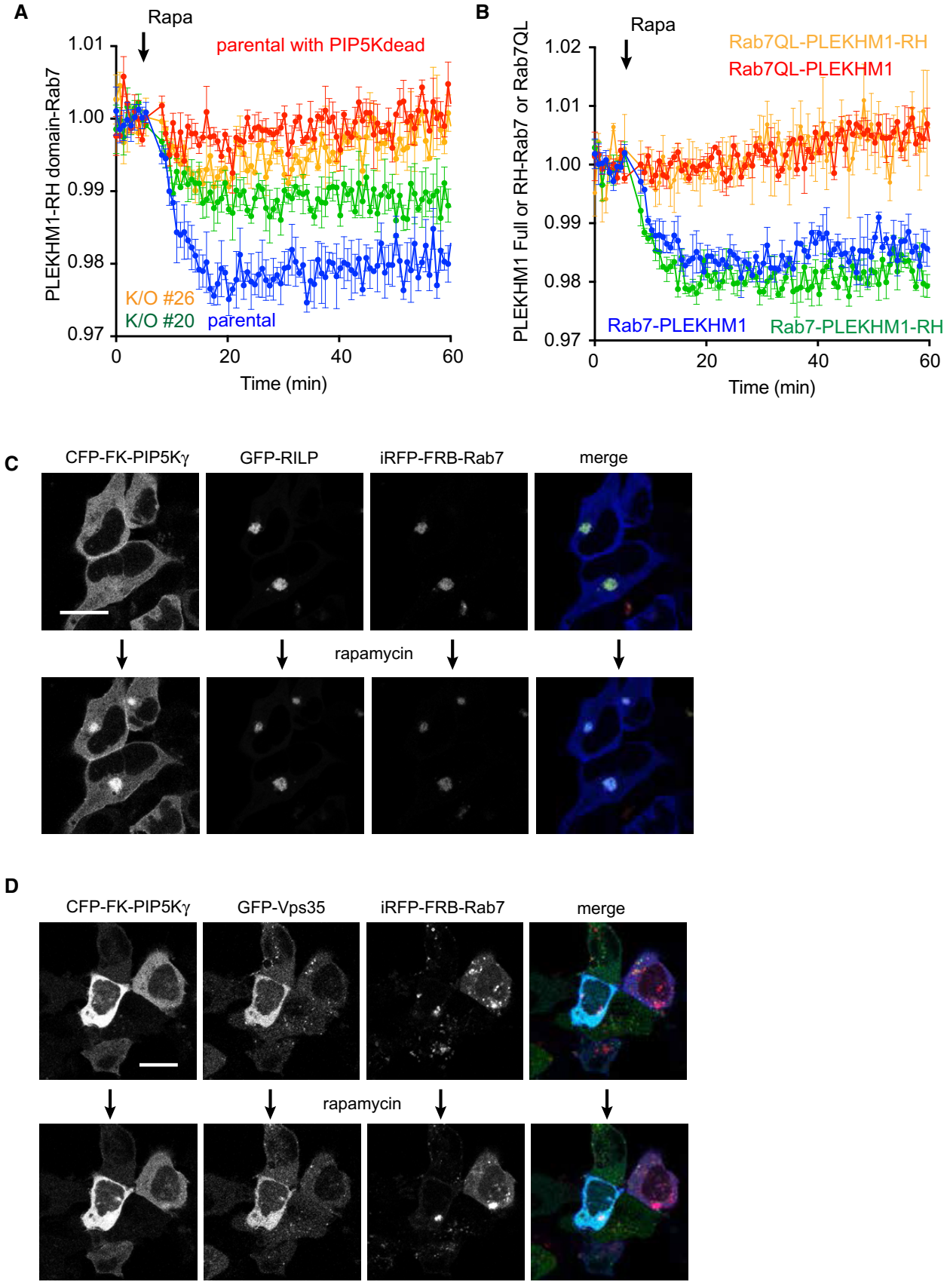

Figure EV4.

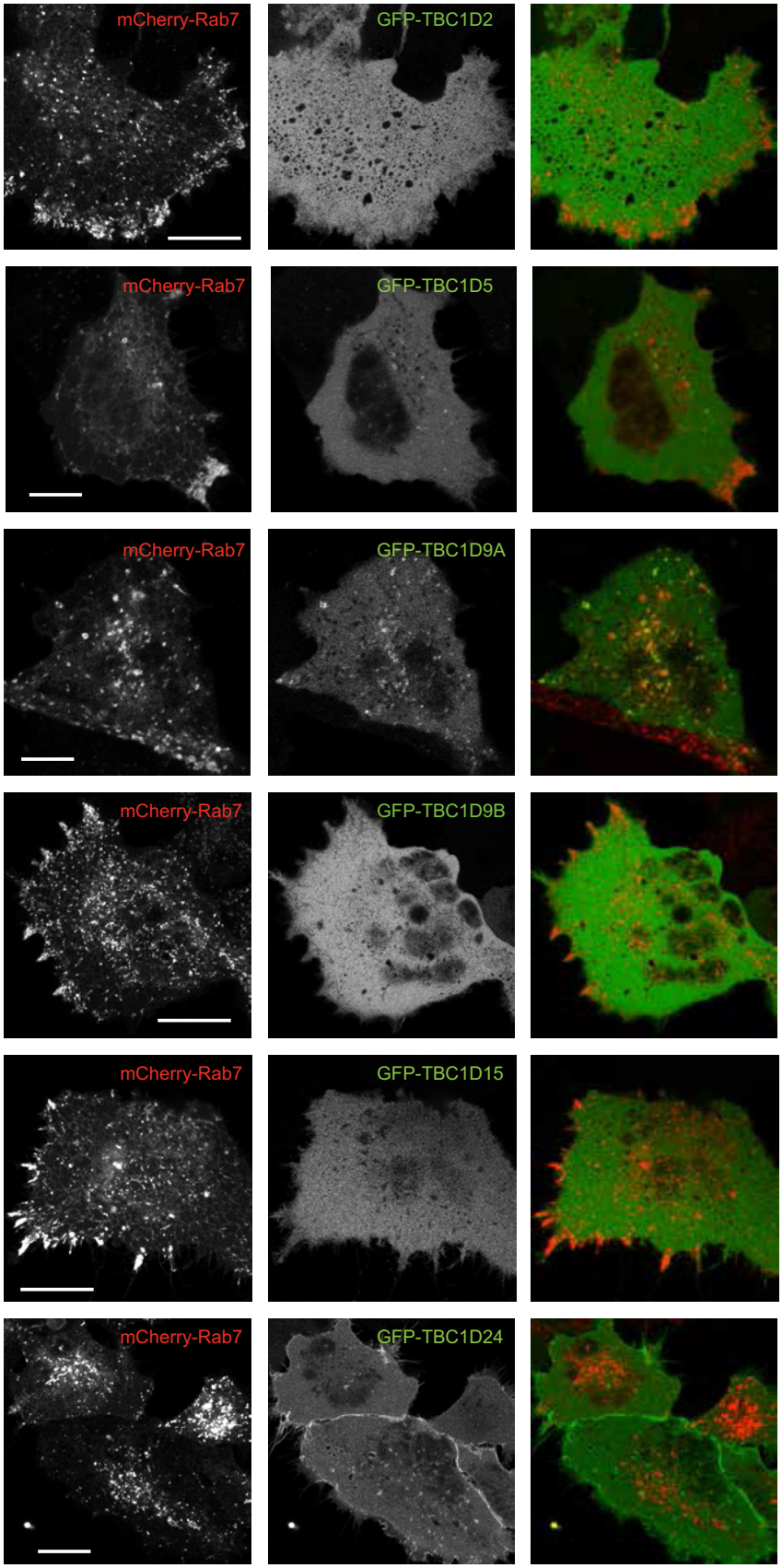

Figure EV5. Distribution of selected GFP-fused TBC1D proteins and mCherry Rab7 co-expressed in HEK293-AT1 cells.
Cells were transfected with the indicated DNAs for 24 h and imaged live by confocal microscopy. Cells expressing low levels of the constructs were chosen to evaluate TBC1D endosomal localization. Note the peripheral distribution of Rab7 after expression of some of the TBC1D proteins. Scale bar: 20 μm.